Thermal and Near Infrared spectroscopic analysis of ZnO, Na_2O, Co_2O_3 and copper oxide of borate glass

Shimaa G. El GABALY [1*], M. E. SULTAN [2], D. A. RAYAN [3,4], F. I. El-HOSINY [5], Y. H. ELBASHAR [6*]

[1] Cairo Higher Institute for Engineering, Computer Science and Management, Cairo, 11865, Egypt

[2] Chemistry Department, Faculty of Science (Boys), Al-Azhar University, Nasr City, Cairo 11884, Egypt

[3] Central Metallurgical Research & Development Institute, P.O. Box: 87, Cairo 11421, Egypt.

[4] Basic Science Department, Faculty of Physical Therapy, Deraya University, Minia,611111, Egypt

[5] Chemistry Department, Faculty of Science, Ain Shams University, Cairo,11566, Egypt.

[6] Basic Science Department, EL Gazeera Higher Institute for Engineering and Technology, Cairo, 11571, Egypt

*Corresponding author: E-mail: y_elbashar@yahoo.com

Abstract

The traditional casting method, bulk glasses with the chemical composition of 55 B_2O_3, 35 ZnO, (10-x) Na_2O, x Co_2O_3, y CuO (x=0, 0.05, 0.1, 0.15, 0.2, 0.25; y=0.1, 0.15, 0.20, 0.25, 0.30, 0.35) were prepared. Differential thermal analysis (DSC) was used to examine the phase shifts and temperature characteristics. It investigated how the various systems' Hruby coefficient, Kauzmann hypothesis Trg= Tg/Tm, glass transition temperature Tg, crystallization temperature Tc, melting temperature Tm, and glass forming ability (Kgl) depended on each other. The structure of the homogenous produced glass networks was examined using the UV-VIS spectroscopic technique for the physical and optical characterization of the glasses, and the XRD technique confirmed the amorphous nature of the glass samples. The density and molar volume of the network were measured using the Archimedes method. Examined and researched were the effects of increasing cobalt and copper oxide concentrations on the manufactured glass samples' optical characteristics, including refractive index, permittivity, extinction coefficient, electric susceptibility, dielectric constants, and optical conductivity. To explore the impact of NIR band-pass glass filters, optical spectroscopy was used to evaluate the glass network over a wavelength range of 190-2500 nm. The glass samples can be categorized as semiconductors.

1. Introduction

Conventional definitions of oxide glasses state that they are networks composed of alkaline oxides (Li_2O, Na_2O, K_2O, ZnO) or alkaline earth oxides (CaO, MgO, SrO) as well as building components such as SiO_2, TeO_2, P_2O_5, B_2O_3, and CdO. When the covalent glass network and oxygen from the metal oxide mix, new structural units are created in these glasses. In most

glass structures, the cations of the modifier oxide encircle the non-bridging oxygen (NBO) [1-3]. Glass materials are among those that are utilized for optical filters the most commonly due to their unique capabilities, which include high transparency, thermal stability, and suitable mechanical and thermo-mechanical properties [4-6]. Transition metal ions are known for their interesting electrical and optical properties. Borate glasses exhibit improved physico-chemical behavior when Cu is added. Under consideration as bandpass filters for several purposes, including sunglass technology and laser protection eyewear, glasses with copper ions in various oxidation states are very beneficial [7-8]. For these kinds of applications, a copper-doped glass former is ideal. Increasing the doping to the near-infrared absorption band can cover the wavelengths of certain lasers, including the YAG laser band at 1064 nm [7]. Transition metal ions, such as copper and cobalt oxides, are present in the glass's matrix in several oxidation or coordination states, giving these glasses unique optical and electrical properties [9]. Examining the effects of simultaneously adding zinc and copper to the glasses would be fascinating [10]. Further improving the glass network's transparency is ZnO. Zinc borate glasses are particularly appealing to scientists. Electrical resistance, chemical stability, and a low coefficient of thermal expansion are just a few of the unusual qualities of these glasses [11]. Aside from their excellent ionic conduction, glassy materials' isotropic qualities and ease of fabrication have drawn a lot of interest as solid electrolytes for solid-state batteries. Borate is a high-quality glass forming. It has a high refractive index along with nonlinear optical properties, chemical stability, and physical stability. The moisture in the air quickly affects it. A specific percentage of planar BO_3 triangles with six members are used to produce borate glass. For the glass, this conduct is unusual. The network structure of the glass under study was found to be mostly composed of BO_3 and BO_4 units arranged in distinct structure groups, with a predominately BO_4 unit, resulting in non-bridging oxygen increases, The melting temperature is typically lowered when B_2O_3 content is increased, while it is typically raised when SiO_2 or Al_2O_3 are added [12-14]. Since transition metal oxide-modified alkali borate glasses have numerous uses in diverse domains, including energy storage technologies, radiation shielding materials, and optical fiber for communication devices, they have emerged as an exciting area of study. Zinc borate glasses are modified by the addition of sodium oxide (Na_2O) at the expense of B_2O_3, which alters the structure and results in modifications to the thermal and physical properties that are the subject of the current study [15]. DSC is frequently used to measure heat capacity, look into thermal stability, and discover phase transitions in the thermal behavior of glasses, polymers, and other materials [16]. Particularly for the creation of photonic glasses like those used in rode and fiberglass lasers, the thermal and thermochemical characteristics of glass are crucial to the fabrication process. The effective optical characteristics, such as emission intensity, can be altered by the glasses' unstable thermal properties [17-18]. The variation in the chemical composition of the glass matrix and its potential impact on the glass transition temperature (Tg), crystallization temperature (Tc), and melting temperature (TM) [17]. The relation for transition temperature Tg, crystallization temperature Tc, and melting temperature Tm is the Hur by coefficient Kgl [19], which is used to calculate the glass's stability or formability. This article examines how copper and cobalt oxides affect the thermal behavior of sodium zinc oxide in borate glass. To characterize the glass samples, the following measurements were made in this study: DSC analysis curves were measured at a rate of 20 C^0/min for the following samples: 55 B2O3, 35 ZnO, (10-x) Na2O, x Co2O3, y CuO (x=0, 0.05, 0.1, 0.15, 0.2, 0.25; y=0.1, 0.15, 0.20, 0.25, 0.30, 0.35 glass activated by different concentrations of Co and Cu ions. Additionally, the difference between the glass transition temperature and glass crystallization was used to calculate the glass formability. Meanwhile, ethanol was used as an immersion fluid

at room temperature to determine the glasses' densities using Archimedes' method. For every glass sample, measurements were taken twice, and averages were calculated. The derived density was used to compute the molar volume. Using room-temperature ethanol as an immersion solvent, the density of each glass sample was determined using the straightforward Archimedes method. The derived density was used to compute the molar volume. The investigation of the bandpass filter with triple bands in the UV, visible, and near-infrared ranges is the basis of this article's uniqueness.

2. **Experimental methods**

2.1. Materials:

ZnO, Na_2CO_3, Co_2O_3, CuO, and H_3BO_3 glass specimens are prepared in powder form using analytical quality raw ingredients. Magnesium oxide (Na_2O) as sodium carbonate powder (Na_2CO_3) (Sigma-Aldrich = 99%), cobalt oxide (Co2O3) (Sigma-Aldrich = 99.99%), copper oxide (CuO) (Sigma-Aldrich = 99.88%), and B2O3 was introduced as boric acid (H_3BO_3) (fluka, purity 99.99%).

2.2. Glass preparation:

Through the use of the glass quenching melting technique, a network of glass with the formula 55 B_2O_3, 35 ZnO, (10-x) Na_2O, x Co_2O_3, y CuO (x=0, 0.05, 0.1, 0.15, 0.2, 0.25; y=0.1, 0.15, 0.20, 0.25, 0.30, 0.35) was prepared for this study. Pure chemical compounds were added, and each sample was ground for 30 minutes using a mortar before being transferred to porcelain crucibles. To release gases such NH_3, H_2O, NO_2, and CO_2, the initial stage involves using a muffle furnace set at 250 c^0. All samples were melted in disposable porcelain crucibles for one hour at 1000 °C using an electrical muffle furnace. To guarantee sample homogeneity and remove gas bubbles, the molten material output was repeatedly shaking [20-23]. Melted components were placed on a heated stainless plate, which was then annealed at 250 °C for 30 minutes using a pressing plate to produce thin disks with a small thickness in millimeters. Samples were then allowed to cool at room temperature to prevent internal stress in the glass samples, and production samples were allowed to cool gradually to room temperature.

2.3. The techniques for characterization:

With a Brucker axis D8 diffractometer and the crystallographic data software Topas 2, the crystallite phase of transparent samples was examined by X-ray diffraction (XRD). The radiation, CuKα (λ = 1.5406 Å), was employed at 40 kV, 30 mA, and 2°/min. For 2θ values between 4° and 70°, the diffraction data were gathered. At room temperature, the Archimedes technique was used to estimate the density, and ethanol was used as the liquid of immersion (density ρ_o= 0.888g/cm³). Eqs. (1, 2) were utilized to ascertain the specimens' density (ρ) and molar volume (Vm), respectively [12,13,22-24].

$$\rho = \frac{W1}{W1-W2}\,\rho \qquad (1)$$

Where w1 and w2 are the weights of samples in air and ethanol, respectively.

$$\mathbf{Vm} = {}^{M\omega}/_{\rho} \qquad (2)$$

2.4 Measurements:

In this study, the glass samples under investigation had their optical absorption and transmission spectra measured at room temperature using a UV/VIS absorption spectrophotometer (JASCO V570) in the wavelength range of 190–2500 nm. Measurements and calculations were made regarding the objects' optical and physical characteristics. Vernier callipers were used to measure the thickness of the matrix sample. Differential Scanning calorimetry (DSC) was performed using the Setaram instrument of Lab-system (TG-DTA-DSC) model 16 with heating rate of 20 c^0/min to a maximum temperature which nearly 1000 C^0 under an inert atmospheric argon gas. To prepare the samples, a small amount of the glass system was ground using an agate mortar. Each sample was then ground into a powder and added to an Aluminum oxide crucible containing 20 mg.

3. Results and discussion

3.1. XRD

XRD spectra of the produced glass network are displayed in Fig. 1. The XRD pattern of the specimens under study indicated that all of the samples had an unstructured temple since there were no distinct peaks required. Thus, neither before nor after the serial addition of metal oxides (Co_2O_3 and CuO) did its amorphous nature change. Conversely, the absence of distinctive metal oxide peaks in XRD patterns for doped glass containing metal oxides is explained by the low concentrations of the metal oxides in the generated glasses.

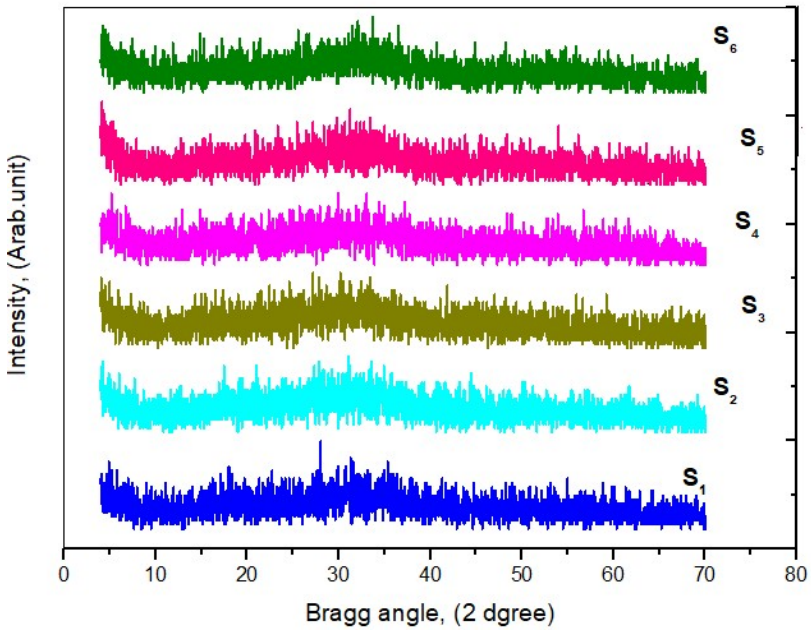

Figure 1. The produced glass specimens' XRD pattern.

3.2 Molar volume & Density:

Glass species' densities and molar volumes were tallied, and Table 1 presents the findings in summary form. The results demonstrated that the glass network of doped Co_2O_3 slightly increases from 2.753 to 2.902 g cm^{-3} with increasing cobalt oxide concentration, whereas the

density of the undoped(S,1) sample of cobalt oxide was the lowest density, equal to 2.753 g cm^{-3}.

Table. 1. Components, density (ρ), molar volume (Vm), (Mw) molar mass.

Samples	Glass components (mol %)					(Mw)*	ρ (g cm^{-3})	Vm ($cm^{-3}mol^{-1}$)
	B_2O_3	ZnO	Na_2O	Co_2O_3	CuO			
S,1	55	35	9.9	0	0.1	71.406	2.753	26.076
S,2	55	35	9.8	0.05	0.15	71.484	2.785	25.747
S,3	55	35	9.7	0.1	0.2	71.561	2.792	25.653
S,4	55	35	9.6	0.15	0.25	71.638	2.805	25.489
S,5	55	35	9.5	0.2	0.3	71.715	2.874	24.866
S,6	55	35	9.4	0.25	0.35	71.791	2.902	24.603

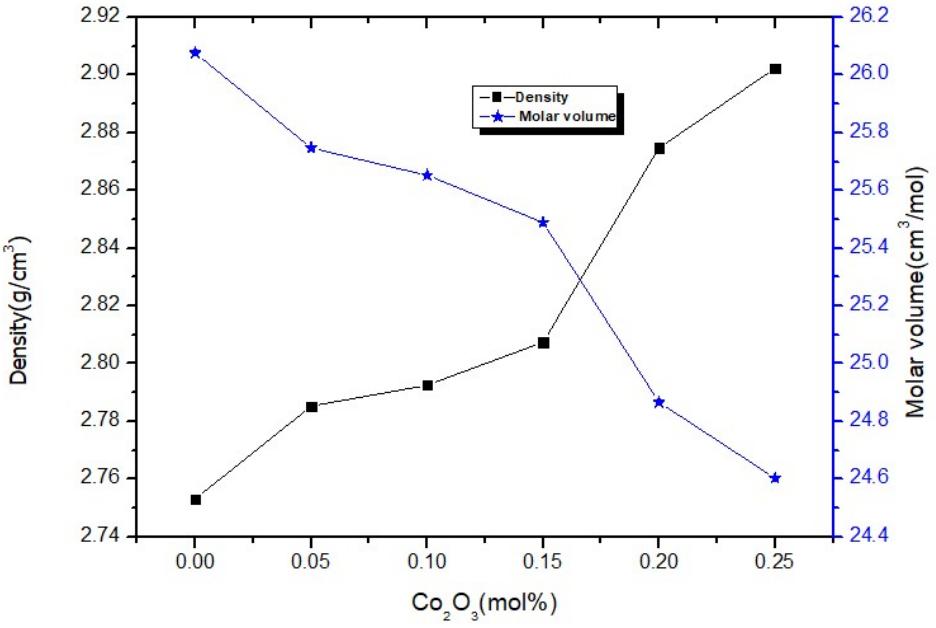

Figure 2. Co_2O_3's effect on the molar volume and density of the glass network fitted.

Because of variations in the atomic weights of Na, Co, and Cu (Fig. 2). Otherwise, as seen in Fig. 2, the molar volume was demonstrated to decrease with increasing cobalt oxide concentration, from 26.076 to 24.603 cm^{-3} mol^{-1}. The borate glass network may undergo structural alterations as a result of the inclusion of CuO and Co_2O_3. These alterations could be

to the atoms' coordination surroundings, bond lengths, or angles. These changes may result in a more compact structure and a drop in molar volume. The larger atomic mass and solid solution formation of cobalt and copper oxides lead to a more densely packed glass structure, which is the main cause of the increase in density and decrease in molar volume of borate glass with increasing concentrations of these oxides [25-26]. These alterations may also be exacerbated by any decrease in porosity and the volume that the additives themselves occupy. Consequently, the presence of Co_2O_3 causes the structure of the doped glass matrix to become less densely packed and raises the degree of disorder, resulting in the formation of an open structure that accounts for the observed increases in density and decreases in molar volume.

3.3. Thermal characteristics:

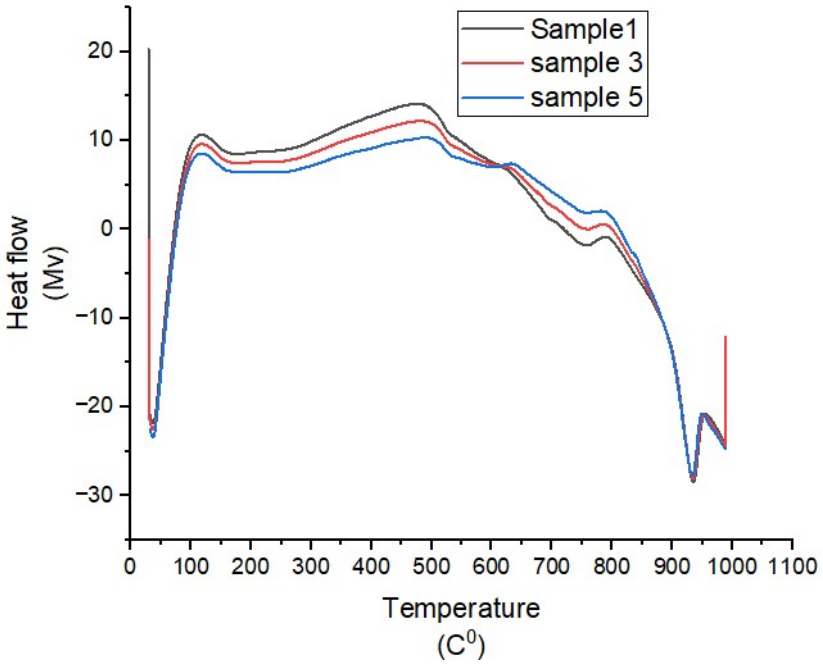

Figure 3 shows the initial curves measured with the DSC for the following variables: x Co2O3, y CuO, (10-x) Na2O, 35 ZnO, and x B2O3 (x=0, 0.1, 0.2; y=0.1,0.20,0.30).

Table 2: The thermal characteristics of x Co_2O_3, y CuO, (10-x) Na_2O, 35 ZnO, and x B_2O_3 (x=0, 0.1, 0.2; y=0.1,0.20,0.30) were determined using DSC at a heating rate of 20 C^0/min.

Samples	Transition temperature (Tg) C^0	Crystallization temperature (Tc) C^0	Melting temperature (Tm) C^0	Kauzmann hypothesis Trg= Tg/Tm	Tm-Tc C^0	ΔT= Tc – Tg C^0	Tm -Tg C^0	glass forming ability (Kgl)	Hurby – parameter Hr
Sample-S1	496.58	758.91	929.74	0.53	170.83	262.33	433.2	0.60	1.53
Sample-S3	485.79	789.57	936.32	0.51	146.75	303.78	450.5	0.67	2.07
Sample-S5	477.26	798.23	942.48	0.50	144.25	320.97	465.2	0.68	2.22

Stability:

According to the Kauzmann hypothesis [27], the forming ability as measured by the parameter Trg = Tg/Tm is found to be in the range of 1/2 ≤ Trg≤ 2/3 [28].
as shown in Table 2. The glass stability is determined by the Hruby parameter [29], which is provided by,

$$Hr = \frac{Tc-Tg}{Tm-} \quad (3)$$

A more stable and interconnected with Hurby – parameter for glass network that is resistant to atom rearrangement and crystalline phase development during heat processing is indicated by a higher Hurby value [31]. The nucleation and growth aspects of phase transformation are combined by this parameter. Greater values of (Tc− Tg) impede the nucleation process, while smaller values of (Tm− Tc) restrain the growth. For HR≤ 0.1, faster quenching rates are necessary; otherwise, standard quenching rates would yield sufficient glass formation [30]. However, it is possible to assess the glass-forming ability utilizing [32]. Ability to produce glass more than 0.6 Thermal stability is useful for applications where the glass must maintain its amorphous structure throughout a range of heat settings [33].

$$\text{glass forming ability (Kgl)} = \frac{Tc-}{Tm-Tg} \quad (4)$$

A declining trend in Tg signifies a weakening of the impact of sodium oxide on the glass matrix, resulting in the development of non-bridging oxygens (NBOs) [34-35]. Tg decreases as the higher dissociation energy B-O bond is being replaced with a lower bond.

3.4. Optical properties:

A useful tool for determining a variety of parameters, including the refractive index, and optical conduction, is the absorption spectra. At room temperature, polished glasses' optical absorption and transmission spectra in the range of 200–2500 nm are measured. The optical absorption spectra of the glass samples for various Co_2O_3 ratios are displayed in Figure 3 spanning the wavelength range of 200–2500 nm. It is evident that as the concentration of Co_2O_3 increases, so does the absorption. Every sample has an optical absorption band in the ultraviolet and visible-near infrared regions, as well as a fundamental optical absorption edge. Figure 5 displays the optical transmission representing the glass samples for various Co_2O_3 ratios in the wavelength range of 200–2500 nm. The absorption values and the transmission spectra agree. In the field of optics, the bandpass technique enables the passage of a band of spectral lines via a filter. It alters if the glasses also include a transition element, the most significant of which are Cu, Ti, V, Cr, Mn, Fe, Co, and Ni. The Ligand-field hypothesis of Hartmann is one of the ideas that explain the phenomenon of coloring. According to this idea, electronic transitions between the energy levels of the electron-degenerate d are responsible for the hue of glasses caused by the transition metals "3d." The transition metal concentration has an impact on the hue as well. There is no doubt about the impact of concentration: as concentration rises, greater absorption results, which reduces transmission [12-13]. Light in the transmission band is attenuated as a result of cobalt oxide replacing $N_{a2}O$, which is why transmission height decreases as the cobalt oxide percentage rises.

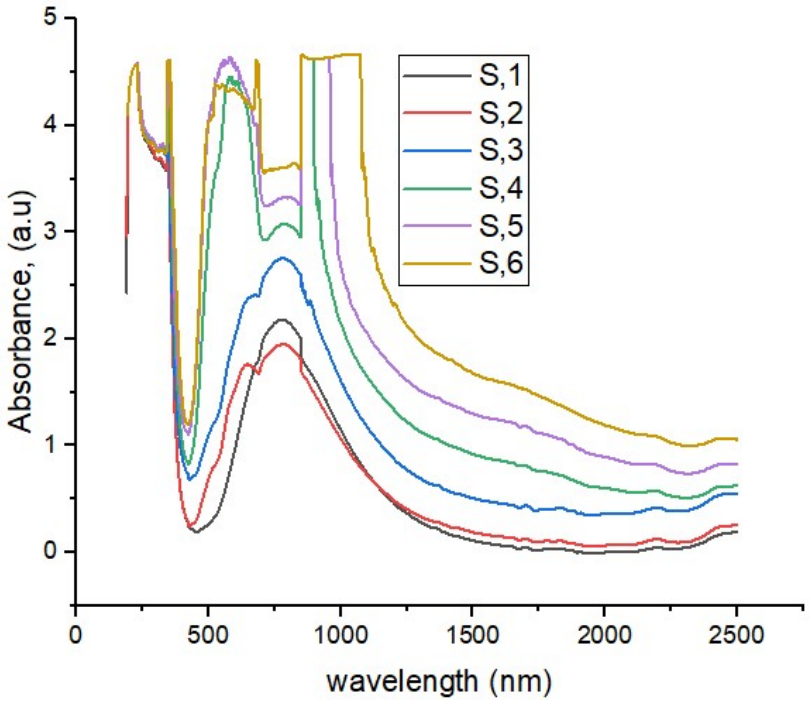

Figure 4. Glass samples' absorption spectra with varying CO_2O_3 contents.

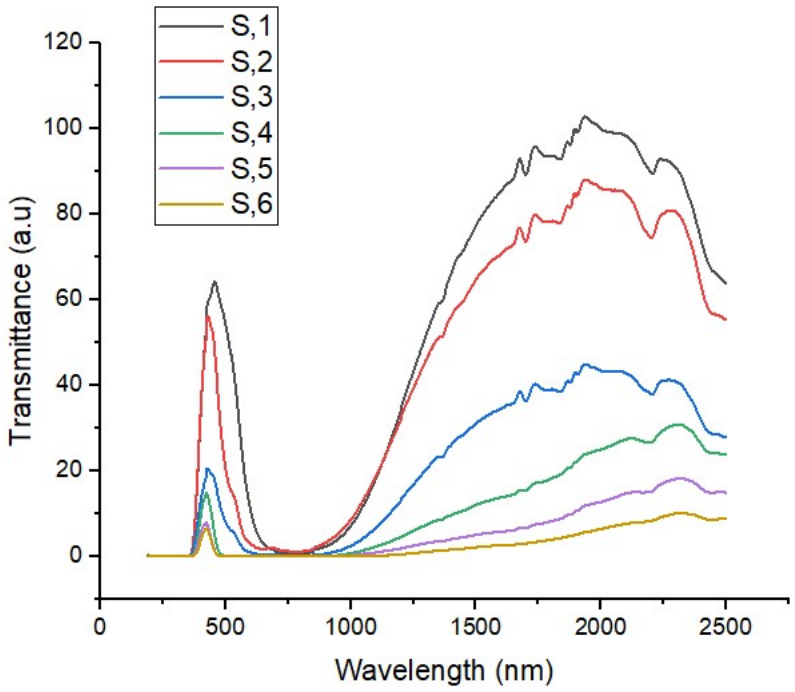

Figure 5. Transmission spectra of glass samples with varying concentrations of Co_2O_3.

Glass's refractive index was determined by many variables, including the characteristics of its constituent parts, the parameters of its oxides, two forms of transmission bridging and non-bridging in the ultraviolet, and the infrared lattice vibration of its specimens [1, 2,12,13]. There were two primary causes for the rise in the refractive index. First of all, Co, Cu, and Na had different ion refractions. Co and Cu doping material had higher ion refraction than Na. Second,

the mean boron separation decreased and the interfacial distance of the glass network shrank when cobalt and copper oxides were added to the glass matrix. As a result, non-bridging oxygen rose, raising the glass samples' refractive index [12,13, 36,37]. This impact is illustrated in Fig. 6.

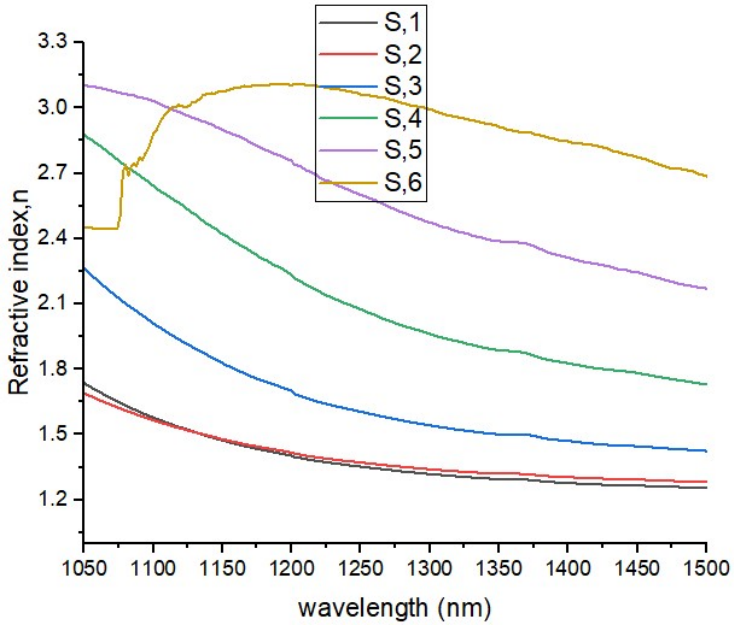

Figure 6. Refractive index wavelength dependence with varying cobalt oxide content.

Permittivity, which was dependent on polarization, electronic transitions, and the vibrations of molecules and atoms in the material, was a measurement of the amount of reduced electric field in a medium relative to a vacuum. Permittivity was found to have two peaks in the ultraviolet and one peak in the infrared. These peaks resulted from doping ions and borate glass absorption resonances, which are connected to electronic transition and energy gaps between levels that are influenced by the glass matrix's composition. Because of their d-d transitions, cobalt, and copper ions both created new absorption bands in the visible and infrared spectrums. Consequently, the permittivity curve tended to move lower in wavelength as the proportion of cobalt and copper oxides rose, having more

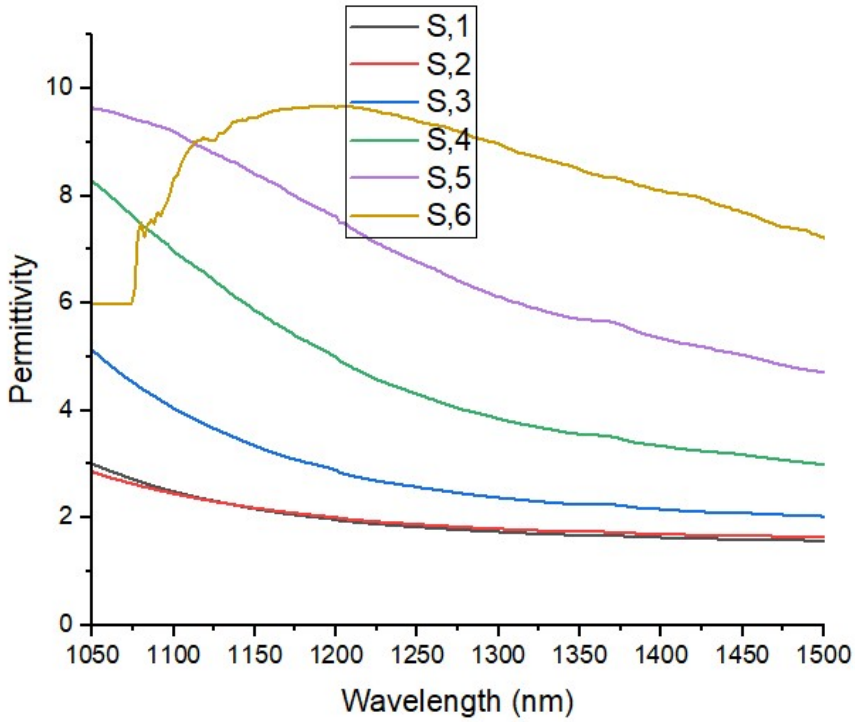

Figure 7. With varying wavelengths, a glass matrix's permittivity changed.

Higher wavelengths caused the glass matrix to become more deformed and depolymerized, which raised the extinction coefficient and vibrational energies [37]. As a result of the glass sample's absorption, the extinction coefficient increases as a doping material increase [38,39], as illustrated in Figure 8.

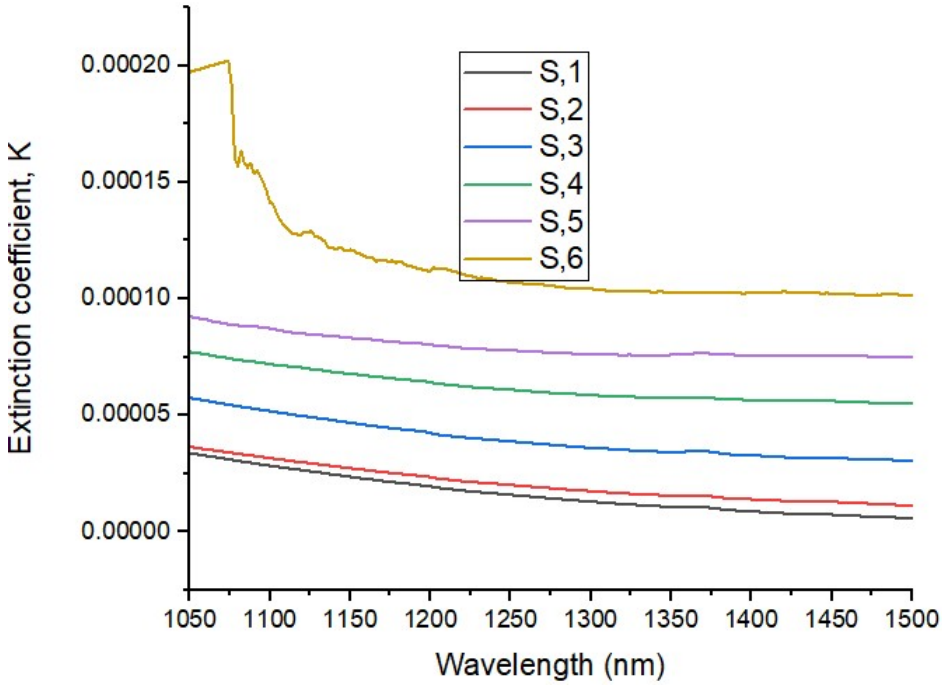

Figure 8. The glass specimens' extinction coefficient, k, as a function of wavelength.

Its ability to be readily polarized by an electric field is known as its electric sensitivity. It was affected by many variables, such as the polarizable entities' characteristics, concentration, and applied electric field wavelength. Because the dopant ions lose some of their ability to polarize the material at longer wavelengths, it may decrease as wavelength increases in some areas of the electromagnetic spectrum. As the concentration of dopant rises, complicated effects on the electric susceptibility might result from interactions between the dopant ions, as illustrated in Figure 9 [40].

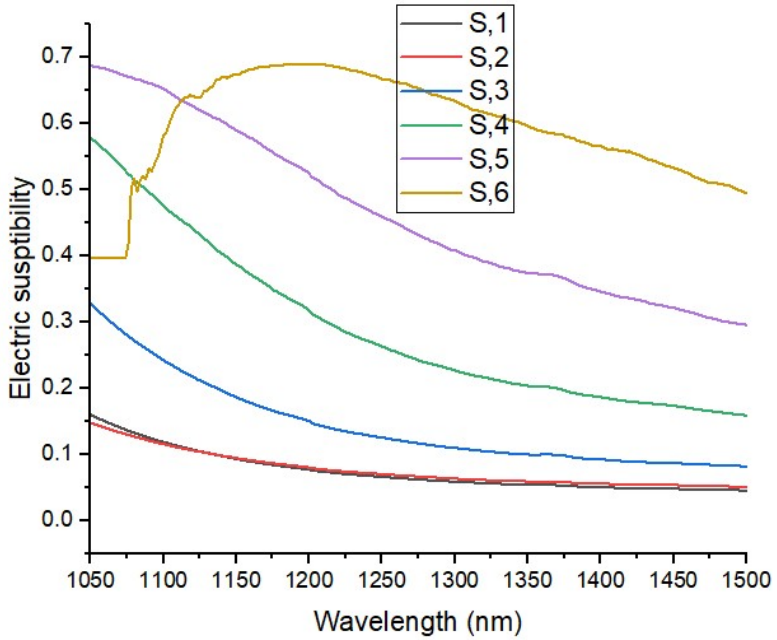

Figure 9. Electric susceptibility as a function of wavelength.

The material's dielectric characteristics were identified via the dielectric and dielectric double constants. The amount of electric charge stored in a material was measured by the dielectric constant, and the amount of electric energy wasted as heat was measured by the dielectric double. Figs. 10 and 11 illustrate how the electric field was absorbed by intense, broad, and overlapped charge transfer transitions at low wavelengths. As a result, the electric field first decreased, then constants with increasing wavelength due to crystal field splitting of d-orbitals, and finally increased due to an increase in vibrational energy [41].

Optical conductivity, when applied to a certain frequency of electric field, is a crucial indicator of a material's capacity to conduct electric current in materials science. The glass matrix's structure and chemical makeup dictated this characteristic. The optical conductivity decreased along with the decrease in transitions that absorb light. The metal ion's d-d transition, which is dependent on the d-orbital crystal field splitting, absorbed the light at intermediate wavelengths. Consequently, the ligand field surrounding the metal ions had an impact on this. Thus, in this area, the optical conductivity doesn't change. As the concentration of copper and cobalt oxides increased, the distorted glass matrix increased, vibrational energy increased, and optical conductivity increased with increasing wavelength [37,42]. The material's optical conductivity was closely correlated with the extinction coefficient, indicating an increase in it [12-13], as shown in Fig.12. This transition related to the stretching and bending mode of borate glass depended on glass composition and modifier of content. as seen in Figure 12.

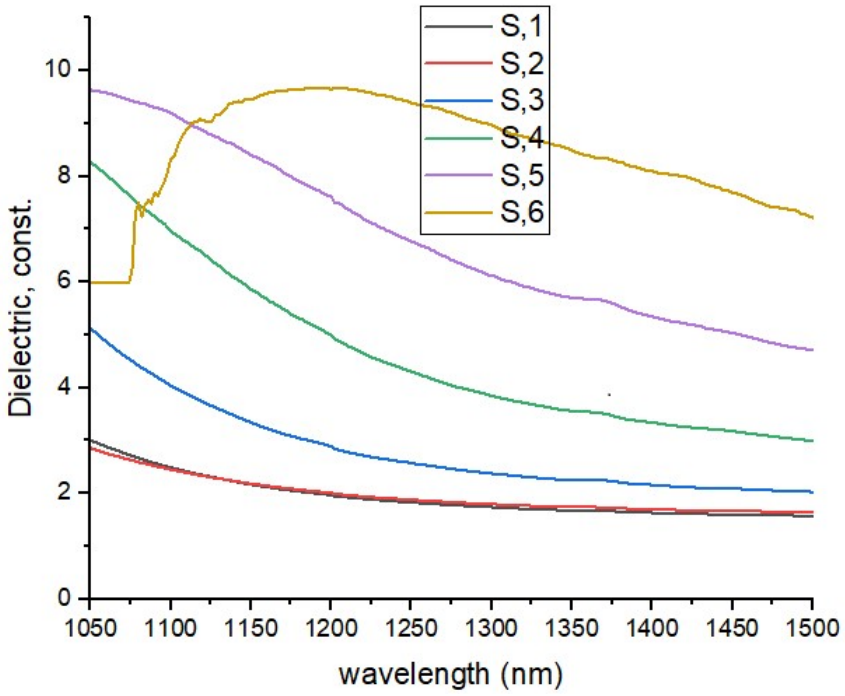

Figure 10. The glass sample dielectric constant is a function of wavelength.

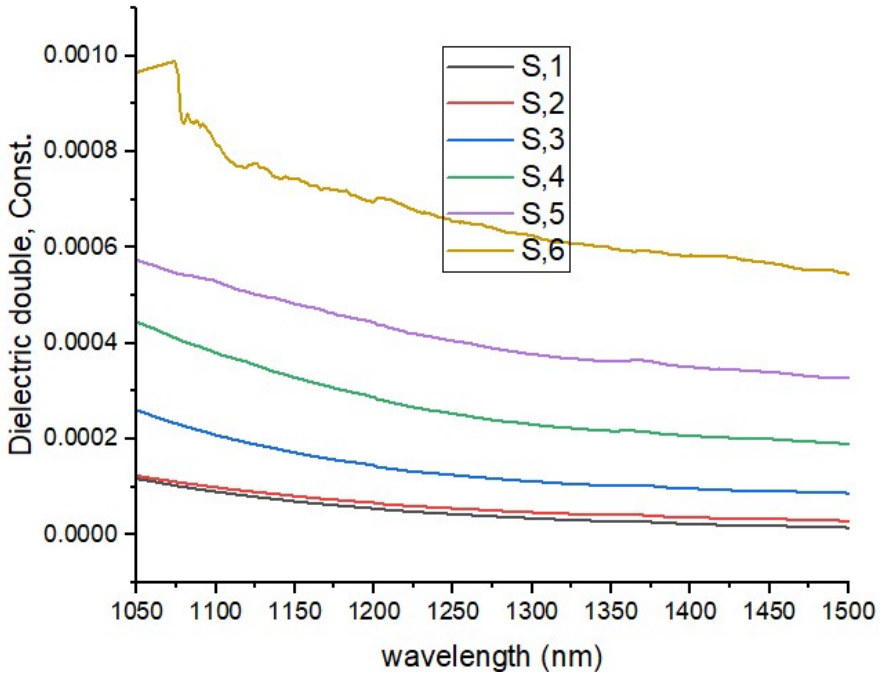

Figure 11. The glass sample dielectric double constant as a function of wavelength.

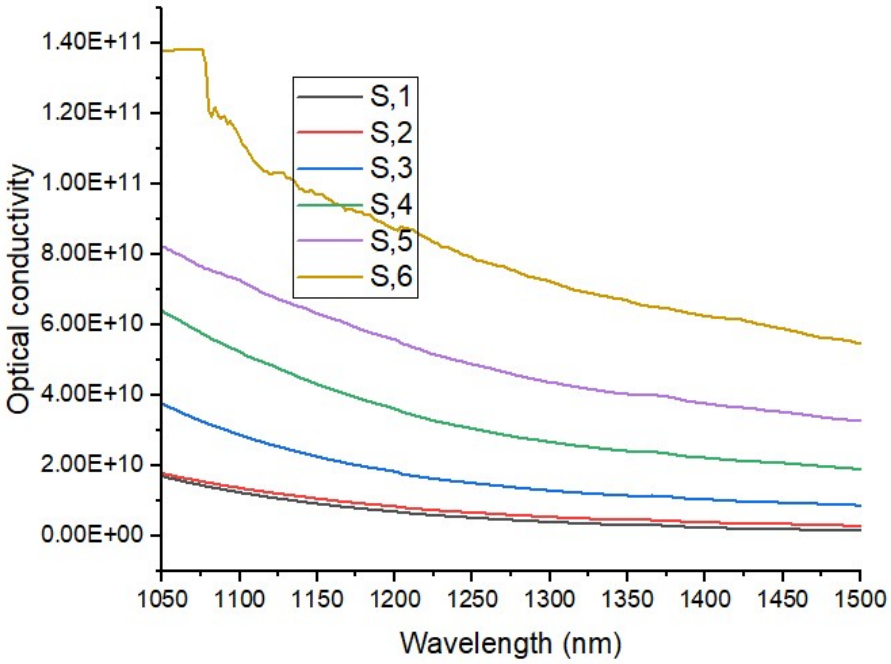

Figure.12. the glass matrix's optical conductivity against wavelength.

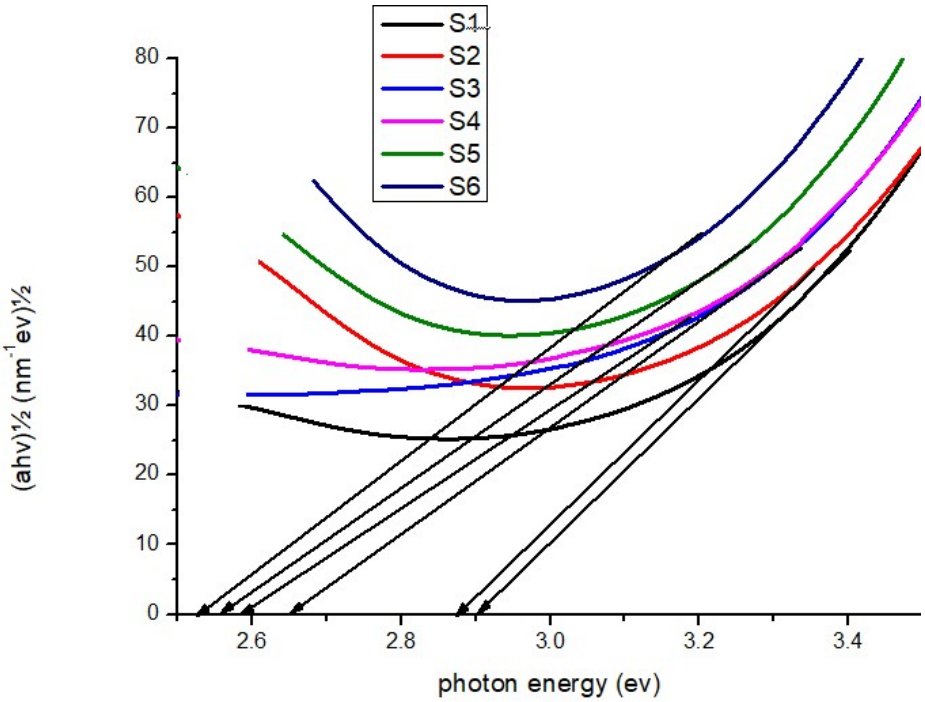

Figure 13. The current glass samples' optical energy gap.

Borate glasses' band gap energy typically ranges from 2.5 to 4.0 electron volts (eV) [43-44], depending on variables like boron oxide content and additional dopants or additives. The plot

of (hωα)1/2 as a function of photon energy (hω) is used to calculate the optical band gap [12-13,36,45] for amorphous materials, as illustrated in fig. 13. The optical band gap of the glass samples, which were thought to be semiconductors in nature, decreased from 2.95 to 2.58 eV due to an increase in the concentration of non-bridging oxygen (NBO) atoms, as demonstrated in figure.13. This decrease was related to the rise in Co_2O_3 and CuO concentricity in the glass. The following relation can be used to compute the refractive index at a given wavelength using reflectance (R) [12-13].

$$\mathbf{R}=\frac{n-1}{n+1} \quad (5)$$

However, the reflectance (R) was counted using the subsequent formula: [12,13,46-48].

$$A + R + T = 1; \text{ So } \quad R = 1 - A - T \quad (6)$$

Where, A: absorbance R: reflectance T: transmittance

Using the following formulas, the permittivity (ε), dielectric const., dielectric double const. and electric susceptibility (χ), of the glass samples were determined [12-13,49-50].

$$\boldsymbol{\varepsilon} = n^2 \quad (7)$$

$$\acute{\varepsilon} = n^2 - k^2 \quad (8)$$

$$\grave{\varepsilon} = 2nk \quad (9)$$

$$\boldsymbol{\chi} = \frac{\varepsilon-1}{4\pi} \quad (10)$$

The extinction coefficient (k) and optical conductivity were calculated by using the following relation [12-13,47-48]

$$k = \frac{\alpha\lambda}{4\pi} \quad (11)$$

$$\text{Optical conductivity} = \alpha nc/4\pi \quad (12)$$

where λ is the wavelength and α is the absorption coefficient.

$$(\alpha\upsilon) = (1/d) \ln (I_o/I) = 2.303\ (A/d) \quad (13)$$

$$a h\upsilon = B\ (h\upsilon - Eg)^2 \quad (14)$$

where α is the computed absorption coefficient using the relation and B is a constant [12-13,47]. where A denotes absorbance and d denotes the thickness of the glass samples, and I_0 and I represent the incident and transmittance beam strengths, respectively.

The glass matrix was employed as an optical band pass filter in the near-infrared range (990-1400 nm), according to the optical results [51-53].

Conclusions

Incorporating Co_2O_3 and CuO into the zinc and sodium oxide glass network was demonstrated in this article. Through the use of XRD, all prepared glass systems are rendered amorphous. The optical band gap energy dropped from 2.95 to 2.58 eV, demonstrating that the glass matrix is a naturally occurring semiconductor. The findings of the experiment demonstrated that the doped material of CuO and Co_2O_3 varied with increasing refractive index, extinction coefficient, permittivity, optical conductivity, electric constant, Dielectric constant, and electric susceptibility. The produced glass network was utilized as NIR optical band pass filter, with a wavelength range of 990–1400 nm, according to the experimental findings. The development of photonic devices, telecommunications, optical storage, and all-optical computing may benefit from the optical reaction that we observed. Optical, DSC, and XRD characterization

measures are used to characterize fabricated glass samples. The concentration of CuO and Co_2O_3 increases significantly, resulting in improvements to both physical and optical qualities.

References

[1] Calahoo, C., & Wondraczek, L. (2020). Ionic glasses: Structure, properties and classification. Journal of Non Crystalline Solids: X, 8, 100054.

[2] Vassilev, Tsvetan, Ivan Penkov, Christina Tzvetkova, and Radost Pascova. "Glass transition temperatures and structures of multicomponent borate glasses: Influence of modifier cation field strengths." *Journal of Non-Crystalline Solids* 438 (2016): 1-6.

[3] Chakraborty, Soumee, L. Herojit Singh, Govind K. Sharma, and T. R. Ravindran. "Understanding alkali oxide induced structural modification at different length-scales in tellurite glasses for improved optical properties." *Journal of Alloys and Compounds* 853 (2021): 156990.

[4] Keshavamurthy, K., and B. Eraiah. "Synthesis, Characterizations and Structural Properties of Rare Earth Doped Bismuth Tellurite Glasses." (2018).

[5] Al-Ghamdi, Hanan, Sabina Yasmin, Mohammad Ibrahim Abualsayed, Ashok Kumar, Aljawhara H. Almuqrin, and Shlair Ibrahim Mohammed. "Influence of the addition of WO3 on TeO2–Na2O glass systems in view of the feature of mechanical, optical, and photon attenuation." *Open Chemistry* 21, no. 1 (2023): 20230136.

[6] TATAR, Demet. "ISTANBUL TECHNICAL UNIVERSITY★ INSTITUTE OF SCIENCE AND TECHNOLOGY." (2011).

[7] Elbashar, Y. H., M. M. Rashad, and D. A. Rayan. "Protection glass eyewear against a YAG laser based on a bandpass absorption filter." *Silicon* 9 (2017): 111-116.

[8] Elbashar, Y. H., S. M. Hussien, J. A. Khaliel, D. I. Moubarak, A. S. Abdel-Rahaman, and H. H. Hassan. "Optical spectroscopic analysis of sodium zinc phosphate glass doped cadmium oxide used for laser window protection." *Annals of the University of Craiova, Physics, Physics AUC* 28 (2018): 57-72.

[9] Elbashar, Y. H., M. A. Mohamed, D. Rayan, A. M. Badr, and H. A. Elshaikh. "Optical spectroscopic analysis of bandpass filter used for laser protection based on cobalt phosphate glass." *Journal of Optics* 49 (2020): 270-276.

[10] Prakash, Amrita Dhara. "Effect of additives on structural and physico chemical properties of alkali borosilicate glass and alternative glass forming systems intended for immobilization of radioactive waste." PhD diss., HOMI BHABHA NATIONAL INSTITUTE, 2021.

[11] Samiei, Sadaf, Ehsan Soheyli, Kunnathodi Vighnesh, Gholamreza Nabiyouni, and Andrey L. Rogach. "Exploring CsPbX3 (X= Cl, Br, I) perovskite nanocrystals in amorphous oxide glasses: innovations in fabrication and applications." *Small* 20, no. 17 (2024): 2307972.

[12] Elbashar, Y. H., Shimaa G. ElGabaly, and D. A. Rayan. "FTIR and NIR spectroscopic analyses of Co3O4-doped sodium zinc borate glass matrix." *Journal of Optics* 50, no. 4 (2021): 559-568.

[13] Elbashar, Yahia, Diaa Rayan, Shimaa ElGabaly, and Adel Mohamed. "Optical spectroscopic study of cobalt oxide doped boron glass and its ion effect on optical properties." *Egyptian Journal of Chemistry* 63, no. 6 (2020): 2111-2124.

[14] Borhan, A. I., Magdalena Gromada, G. G. Nedelcu, and L. Leontie. "Influence of (CoO, CaO, B2O3) additives on thermal and dielectric properties of BaO–Al2O3–SiO2 glass–ceramic sealant for OTM applications." *Ceramics International* 42, no. 8 (2016): 10459-10468.

[15] Shirif, M. A., M. Medhat, S. Y. El-Zaiat, A. M. Fayad, and F. A. Moustafa. "Optical properties of silver halide photochromic glasses doped with cobalt oxide." *Silicon* 10 (2018): 219-227.

[16] Zheng, Qiuju, Yanfei Zhang, Maziar Montazerian, Ozgur Gulbiten, John C. Mauro, Edgar D. Zanotto, and Yuanzheng Yue. "Understanding glass through differential scanning calorimetry." *Chemical reviews* 119, no. 13 (2019): 7848-7939.

[17] Zhang, Yan, Chunhua Lu, Yijun Feng, Liyan Sun, Yaru Ni, and Zhongzi Xu. "Effects of GeO2 on the thermal stability and optical properties of Er3+/Yb3+-codoped oxyfluoride tellurite glasses." *Materials Chemistry and Physics* 126, no. 3 (2011): 786-790.

[18] Elbashar, Y. H., and D. A. Rayan. "Thermal analysis of B2O3-Na2O-ZnO glass doped Nd2O3." *International Journal of Applied Engineering Research (IJAER)* 11, no. 8 (2016): 5791-5796.

[19] Reddy, C. Narayana, and RP Sreekanth Chakradhar. "Elastic properties and spectroscopic studies of fast ion conducting Li2OZnOB2O3 glass system." *Materials research bulletin* 42, no. 7 (2007): 1337-1347.

[20] Elbashar, Y. H., M. A. Mohamed, A. M. Badr, H. A. Elshaikh, and Diaa A. Rayan. "X-ray spectroscopic analysis of nanocrystal phase growth in cobalt oxide-doped copper zinc sodium phosphate glass matrix." *Journal of Optics* 50 (2021): 253-256.

[21] Abu-Khadra, Ahmad S., Ashraf M. Taha, A. M. Abdel-Ghany, and Ashraf A. Abul-Magd. "Effect of silver iodide (AgI) on structural and optical properties of cobalt doped lead-borate glasses." *Ceramics International* 47, no. 18 (2021): 26271-26279.

[22] Elbashar, Y. H., and H. A. Abd El-Ghany. "Optical spectroscopic analysis of Fe 2 O 3 doped CuO containing phosphate glass." *Optical and Quantum Electronics* 49 (2017): 1-13.

[23] Krol, Igor, Roman Avetisov, Marina Zykova, Ksenia Kazmina, and Olga Barinova. "Zinc borosilicate glasses doped with Co2+ ions: Synthesis and optical properties." *Optical Materials* 132 (2022): 112768.

[24] Elbashar, Y. H., DIAA RAYAN, SHIMAA G. ELGABALY, and A. A. Mohamed. "The Effect of Cobalt Ions on Boron Glass: A Review." *Nonlinear Optics, Quantum Optics: Concepts in Modern Optics* 54 (2021).

[25] Smiljanić, Sonja, Snežana Grujić, Mihajlo B. Tošić, Vladimir D. Živanović, Srđan D. Matijašević, Jelena D. Nikolić, and Vladimir S. Topalović. "Effect of La2O3 on the structure and the properties of strontium borate glasses." *Chemical Industry & Chemical Engineering Quarterly* 22, no. 1 (2016): 111-115.

[26] Abdel-Ghany, A. M., Ahmad S. Abu-Khadra, and M. S. Sadeq. "Influence of Fe cations on the structural and optical properties of alkali-alkaline borate glasses." *Journal of Non-Crystalline Solids* 548 (2020): 120320.

[27] Kauzmann, Walter. "The nature of the glassy state and the behavior of liquids at low temperatures." *Chemical reviews* 43, no. 2 (1948): 219-256.

[28] Clavaguera-Mora, M. T. "Glassy materials: thermodynamic and kinetic quantities." *Journal of alloys and compounds* 220, no. 1-2 (1995): 197-205.

[29] Hrubý, AJCJoPB. "Evaluation of glass-forming tendency by means of DTA." *Czechoslovak Journal of Physics B* 22, no. 11 (1972): 1187-1193.

[30] Y.H.Elbashar, "Structural and spectroscopic analyses of copper doped P2O5-ZnO-K2O-Bi2O3 glasses", Proces. Appl. Ceram., 9 [3] (2015) 169–173.

[31] Kumar, Amit, S. S. Fouad, M. S. El-Bana, and Neeraj Mehta. "Thermal analysis of cadmium addition on the glass transition and crystallization kinetics of Se–Te–Sn glassy network." *Journal of Thermal Analysis and Calorimetry* 131, no. 3 (2018): 2491-2501

[32] Shaaban, Essam R., and S. H. Mohamed. "Thermal stability and crystallization kinetics of Pb and Bi borate-based glasses." *Journal of thermal analysis and calorimetry* 107, no. 2 (2012): 617-624.

[33] Yu, Lian. "Surface mobility of molecular glasses and its importance in physical stability." *Advanced drug delivery reviews* 100 (2016): 3-9.

[34] Bala, Manju, Suman Pawaria, Nisha Deopa, Sajjan Dahiya, Anil Ohlan, R. Punia, and A. S. Maan. "Structural, optical, thermal and other physical properties of Bi2O3 modified Lithium Zinc Silicate glasses." *Journal of Molecular Structure* 1234 (2021): 130160.

[35] Ahlawat, J., Suman Pawaria, Manju Bala, Sajjan Dahiya, Anil Ohlan, R. Punia, and A. S. Maan. "Study of thermal and physical properties of sodium modified zinc borate glasses." *Materials Today: Proceedings* 79 (2023): 118-121.

[36] S. S. Moslem, Yahia.H.Elbashar, Diaa.A. Rayan, Hussam. H. Hassan, "Double Bandpass Absorption Glass Filter: A review" , Journal of nonlinear optics and quantum optics, NLOQO Volume 53, Number 3-4 (2021), 209-273

[37] Abdel-Baki, Manal, F. A. Abdel-Wahab, Amr Radi, and Fouad El-Diasty. "Factors affecting optical dispersion in borate glass systems." *Journal of Physics and Chemistry of Solids* 68, no. 8 (2007): 1457-1470.

[38] Marzouk, Samir Y., Roshdi Seoudi, Doaa A. Said, and Mai S. Mabrouk. "Linear and non-linear optics and FTIR characteristics of borosilicate glasses doped with gadolinium ions." *Optical Materials* 35, no. 12 (2013): 2077-2084

[39] Abdel-Ghany, A. M., Ahmad S. Abu-Khadra, and M. S. Sadeq. "Influence of Fe cations on the structural and optical properties of alkali-alkaline borate glasses." *Journal of Non-Crystalline Solids* 548 (2020): 120320.

[40] Sallam, O. I., A. Abdel-Galil, and N. L. Moussa. "Tuning of smart cobalt doped borate glasses by electron beam as band-pass filters." *Optics & Laser Technology* 162 (2023): 109262.

[41] Al Kiey, Sherief A., Rania Ramadan, and Mai M. El-Masry. "Synthesis and characterization of mixed ternary transition metal ferrite nanoparticles comprising cobalt, copper and binary cobalt–copper for high-performance supercapacitor applications." *Applied Physics A* 128, no. 6 (2022): 473.

[42] Gomaa, Hosam M., Ahmad S. Abu-Khadra, H. Algarni, I. S. Yahia, H. Y. Zahran, and A. M. Abdel-Ghany. "Effect of BaO doping on the structural and optical properties of some cerium-copper sodium borate glasses." *Journal of the Australian Ceramic Society* 59, no. 2 (2023): 343-353

[43] Zandonà, Alessio, Victor Castaing, Alexander I. Shames, Gundula Helsch, Joachim Deubener, Ana Isabel Becerro, Mathieu Allix, and Adrian Goldstein. "Oxidation and coordination states assumed by transition metal dopants in an invert ultrabasic silicate glass." *Journal of Non-Crystalline Solids* 603 (2023): 122094.

[44] Yahia.H.Elbashar, D. A. Rayan, Hedra Emad R. Saleh, Roshdy A. AbdelRassoul, " Optical Spectroscopic Analysis of Neodymium Oxide Doped Phosphate Glass Matrix for Solar Energy Applications", Journal of nonlinear optics and quantum optics, NLOQO Volume 53, Number 3-4 (2021), 275-289

[45] Abdel-Gayed, M. S., Y. H. Elbashar, M. H. Barakat, and M. R. Shehata. "Optical spectroscopic investigations on silver doped sodium phosphate glass." *Optical and Quantum Electronics* 49 (2017): 1-12.

[46] D.A. Rayan, Y.H.Elbashar, S.S. Moslem, "ESR and magnetic studies of nickel ions doped P2O5–ZnO–Na2O glassy system", Revista Mexicana de Fisica , Vol 66, No 5 Sept-Oct (2020), 580-584

[47] Abouhaswa, A. S., Y. S. Rammah, S. E. Ibrahim, and A. A. El-Hamalawy. "Structural, optical, and electrical characterization of borate glasses doped with SnO2." *Journal of Non-Crystalline Solids* 494 (2018): 59-65.

[48] Sreenivasulu, M., and Vijaya Kumar Chavan. "Optical applications of transition metal ion doped phosphate glasses." *Physica Scripta* 96, no. 12 (2021): 125876.

[49] Ahmad, F., E. Hassan Aly, M. Atef, and M. M. ElOkr. "Study the influence of zinc oxide addition on cobalt doped alkaline earth borate glasses." *Journal of alloys and compounds* 593 (2014): 250-255.

[50] Rayan, D. A., Y. H. Elbashar, M. M. Rashad, and A. El-Korashy. "Optical spectroscopic analysis of cupric oxide doped barium phosphate glass for bandpass absorption filter." *Journal of Non-crystalline solids* 382 (2013): 52-56

[51] Abu-Raia, W. A., D. A. Aloraini, S. A. El-Khateeb, and Aly Saeed. "Ni ions doped oxyflourophosphate glass as a triple ultraviolet–visible–near infrared broad bandpass optical filter." *Scientific Reports* 12, no. 1 (2022): 16024.

[52] Ikehata, Akifumi. "NIR optics and measurement methods." *Near-infrared spectroscopy: Theory, spectral analysis, instrumentation, and applications* (2021): 211-233.

[53] Banoqitah, Essam, Fathi Djouider, Essam B. Moustafa, and Ahmed H. Hammad. "Copper-containing barium zinc borophosphate glass bandpass filters: structural and optical investigations." *Optical and Quantum Electronics* 54, no. 11 (2022): 759.